M&C 2017 - International Conference on Mathematics & Computational Methods Applied to Nuclear Science & Engineering, Jeju, Korea, April 16-20, 2017, on USB (2017)

Analyzing the BEAVRS HZP case with KMACS using 2-group data from SCALE-NEWT, HELIOS and nTRACER

Matías Zilly, Jérémy Bousquet, Kiril Velkov*, Young Suk Ban, Han Gyu Joo†

*Gesellschaft für Anlagen- und Reaktorsicherheit (GRS) gGmbH, Boltzmannstraße 14, 85748 Garching, Germany
†Department of Nuclear Engineering, Seoul National University, 599 Gwanak-ro, Gwanak-gu, Seoul 151-744, Korea
matias.zilly@grs.de

Abstract - *Up until now, the GRS core simulator KMACS has applied 2-group data produced by SCALE-NEWT. Making use of its modular concept, now also nTRACER and HELIOS can be used as lattice codes within KMACS. This paper presents first results for this new functionality. Considering the BEAVRS first core at HZP conditions, nodal core results based on the three lattice codes are compared with measurement data and reference calculations. Results for the HZP eigenvalues, radial power distributions, control bank worths and isothermal temperature coefficients are presented. Specially the KMACS-nTRACER results are very close to the reference.*

I. INTRODUCTION

While direct whole-core simulation is becoming state of the art in steady-state analysis for light-water power reactors, the traditional 2-step approach of generating functionalized few-group data with a lattice code and then using them in a nodal code remains the tool of choice for production applications, as well as uncertainty and transient analyses.

For verification and validation purpose, each code sequence (lattice code/nodal code) has to be compared to reference calculations and experimental data.

The GRS core simulator KMACS [1] combines lattice code, nodal diffusion code with explicit thermal-hydraulics feedback and inventory code into a nodal core simulator. The individual codes are steered and executed via Python modules. The results are stored into a central data base which also serves for data exchange and analysis.

Within KMACS, the SCALE-NEWT/QUABOX-CUBBOX sequence has been validated against operational data of various German PWR reactor cycles [2], and also within an international cooperation with IRSN, France [3]. Using NEWT [4], the lattice calculations are the most time-consuming part of the core simulation. Furthermore, from a scientific point of view, it is worth to study the impact of the choice of the lattice code on the core simulator results.

Therefore, the two additional lattice codes nTRACER and HELIOS have been added as options into KMACS.

The MOC code nTRACER [5], developed at Seoul National University, is a validated direct whole-core simulator. Recently, it has been extended by a routine to generate few-group constants through assembly lattice calculations [6].

Studsvik Scandpower's HELIOS [7] is a widely used and well-validated lattice code based on the current-coupling and collision probability method. It allows flexible geometry, including hexagonal lattices, and consumes far less computational resources compared to NEWT and nTRACER.

This paper contains a comparison of KMACS using nTRACER (rev. 551, ENDF-B/VII-based 47 group library), HELIOS 1.12 (ENDF-B/VI 47-group adjusted library), and SCALE6.2.1-NEWT (ENDF-B/VII.1 56 group library) 2-group data on the one hand, with measurement and SERPENT Monte-Carlo (version 2.1.25, ENDF-B/VII.0 continuous energy) as well as nTRACER reference calculations on the other hand.

The system under examination is the BEAVRS PWR reactor at beginning of life (BOL) hot zero power (HZP) conditions, according to the benchmark specification rev. 1.1.1 [8]. As the thermal-hydraulic state is fixed and only fresh fuel is present, this choice allows a study of the pure lattice-code effect on the core simulation.

The comparisons comprise the eigenvalues, control rod worths, radial power distributions, and isothermal temperature coefficients.

II. MODEL OF THE BEAVRS CORE

1. BEAVRS reactor and HZP conditions

The reactor addressed in the BEAVRS benchmark is a four-loop Westinghouse PWR loaded with 193 fuel assemblies of 17×17 lattice with a rated power of 3411 MWth. All assemblies contain fresh UO_2 fuel in three different enrichments, 1.6%, 2.4%, 3.1% U-235. Excess reactivity in the core is limited by burnable absorbers in form of boron glass rods which are inserted into guide tubes at certain core positions.

The benchmark specification provides all detailed geometrical data and material compositions for the major core constituents including the assemblies, baffle and the barrel. Also the location, composition and geometry of the spacer grids is specified. The benchmark hot zero-power core conditions are listed in Table I.

TABLE I. Key reactor parameters at HZP conditions.

Power	25 MWth
Pressure	15.51 MPa
Temperature	566.5 K
Moderator density	0.73986 g/cm^3
Boron concentration	975 ppm

2. Reference full core models

Two reference full-core models have been considered. A SERPENT model for the core without control rods, and a

nTRACER model for the rodded configurations.

A. SERPENT model

For the reference calculations using SERPENT, the core was modeled in full detail as described in [8]. As a simplification, empty guide tubes were placed at all instrumentation tube positions. Thus there is a 1/8th core symmetry. No control rods (CR) are present in the model. Figure 1 illustrates the SERPENT core model.

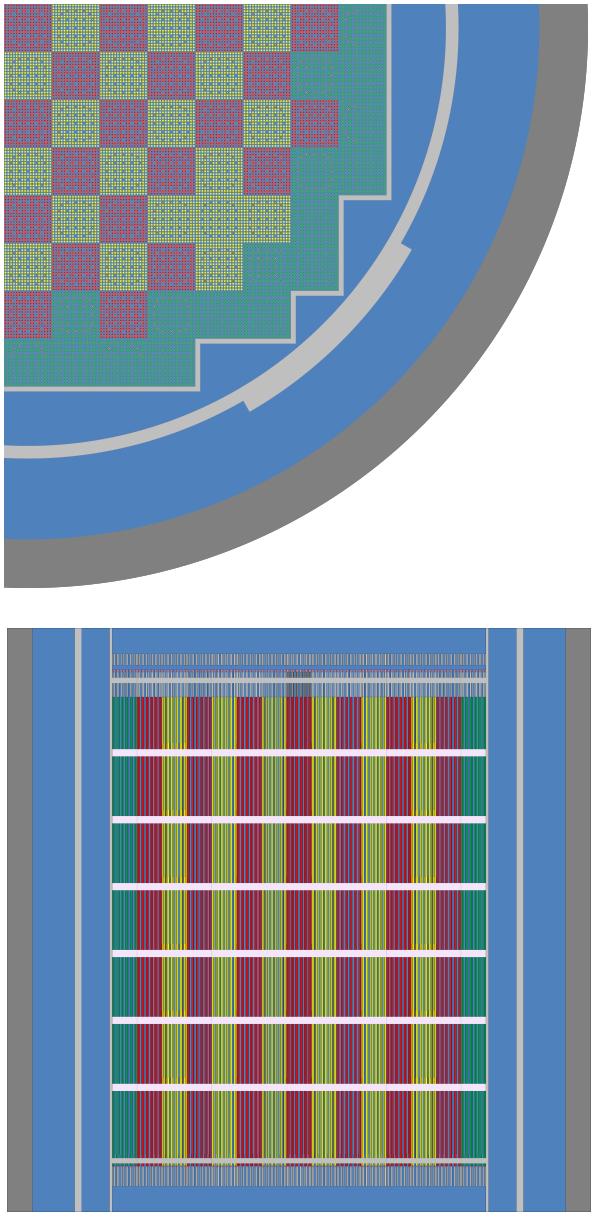

Fig. 1. Horizontal and vertical section of the SERPENT reference model.

The red, yellow, and green colored fuel corresponds to 1.6%, 2.4%, and 3.1% enriched UO_2. Bright points within the fuel assembly guide tubes depict the boron glass burnable absorber rods. The baffle and core barrel, including the neutron shield, are depicted in light gray. The pressure vessel (dark gray) delimits the model. In the vertical section, also the positions of the spacer grids can be recognized, the brighter being Zircaloy grids, the darker stainless steel/Inconel grids.

B. nTRACER model

The nTRACER reference model is the one from [9], and described in full detail therein. It is consistent with the SERPENT model with two minor differences. The reactor pressure vessel is not part of the model. Furthermore, the spacer grids are modeled as smeared metal/moderator zones at the corners of each pin cell at their exact axial positions. A sensitivity study in [9] has shown that both model simplifications have a negligible effect on the quantities considered here.

3. KMACS: Generation of 2-group data

For the 2-group data generation, 2d-transport calculations were performed for 1/4-assemblies with reflective boundary conditions. The 3.1% enriched assemblies which contain 6 and 15 burnable absorber (BA) rods are not mirror-symmetric with respect to the assembly mid plane. Therefore, 2 and 3 different lattices for these assemblies are considered, respectively. Due to the reflective boundary conditions, the resulting lattices contain 12 and 0 BA rods (6 BA assemblies), and 24, 14, and 8 BA rods (15 BA assemblies).

In order to allow for a regular axial nodalization, all spacer grids of the active zone were smeared homogeneously into the moderator in between the fuel pins and guide tubes as well as the inter-assembly gap. On the other hand, the moderator within the guide tube was modeled without structure materials. Assuming a single geometry for the guide tubes ("above dashpot"), in this results in 11 unique lattices, 3 of which have a controlled status (CR=1). Here, these lattices are denoted by enrichment, number of burnable absorber rods, and control status, e.g. 3.1-12/0. Cf. Table II.

TABLE II. Nomenclature of the lattices.

Enrichment	BA rods	CR	Quadrant	Lattice
1.6%	0	0		1.6-0/0
1.6%	0	1		1.6-0/1
2.4%	0	0		2.4-0/0
2.4%	0	1		2.4-0/1
2.4%	12	0		2.4-0/12
2.4%	16	0		2.4-0/16
3.1%	0	0		3.1-0/0
3.1%	0	1		3.1-0/1
3.1%	6	0	NW	3.1-12/0
3.1%	12	0		3.1-12/0
3.1%	15	0	NW	3.1-24/0
3.1%	15	0	NE	3.1-14/0
3.1%	15	0	SE	3.1-8/0
3.1%	16	0		3.1-16/0
3.1%	20	0		3.1-20/0

The nomenclature of the quadrants is according to the figures in the benchmark description. Quadrants of the asymmet-

ric lattices which are not mentioned in the table are identical or mirror-symmetric to other lattices. Some of the lattices are depicted in Figure 2. For their arrangement in the core, see Figure 3.

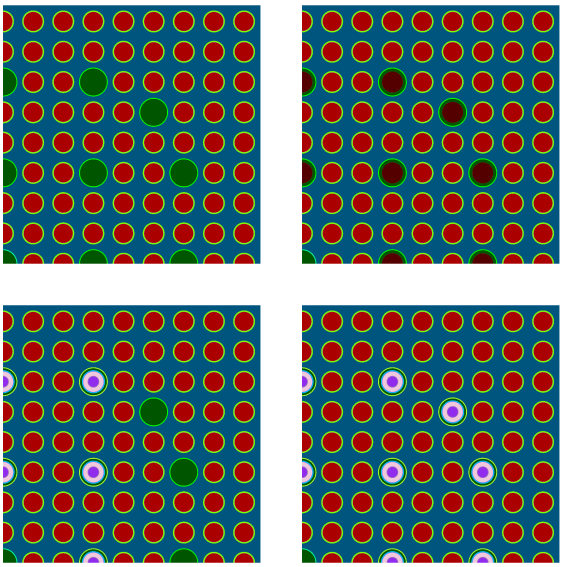

Fig. 2. SCALE-Fulcrum visualization of the lattices 3.1-0/0, 3.1-0/1 (above), 3.1-14/0, and 3.1-24/0 (below).

KMACS automatically generates consistent inputs for the three applied transport codes SCALE-NEWT, HELIOS and nTRACER with identical isotopics and temperatures, executes the codes and stores the resulting 2-group data in a database.

The 2-group data required for each lattice in order to run QUABOX/CUBBOX [10] as nodal code within KMACS are the following: $\mathtt{D}_{1,2}$, $\mathtt{ABS}_{1,2}$, $\mathtt{FIS}_{1,2}$, $\mathtt{Nu\text{-}F}_{1,2}$, $\mathtt{Kap\text{-}F}_{1,2}$, $\mathtt{REM}$.[1] The quantities indexed with $\mathtt{1,2}$ correspond to the usual macroscopic diffusion constant, absorption, fission, neutron production, and energy release cross sections in the fast and thermal energy group. $\mathtt{REM}$ is the macroscopic fast to thermal downscattering cross section. For consistency, the latter quantity has to be corrected if thermal upscattering is present. In QUABOX/CUBBOX, assembly discontinuity factors (ADF) are taken into account by dividing the 2-group data by the respective ADF [11], e.g. $\mathtt{D}_1 \rightarrow \frac{\mathtt{D}_1}{\mathtt{ADF}_1}$. This implies that direction-dependent ADF cannot be taken into account using QUABOX/CUBBOX. Therefore, the arithmetic mean value of the ADFs produced for each lattice is used.

For the present study, the following thermal-hydraulic states were considered as branch states, cf. Table III.

The HZP all-rods out (ARO) parameters as nominal state are indicated in bold font. For HZP conditions, the power generation is considered to be negligible. Therefore equal fuel and moderator temperature $T_{\text{fuel}} = T_{\text{moderator}}$ is assumed. The moderator densities listed in Table III correspond to the isobaric conditions of water at a nominal pressure and hot zero temperature, and temperatures ±10°F= ±5.56 K, according to [12]. Together with the listed boron concentrations, all thermal-hydraulic states defined for the hot zero power physics tests in the benchmark can be represented.

[1] Xenon cross-sections are irrelevant for the fresh core.

TABLE III. List of thermohydraulic states considered for the 2-group data generation.

T_{fuel} [K]	ρ_{mod} [g/cm^3]	c_{Bor} [ppm]
560.9	0.75037	**975**
566.5	**0.73986**	902
572.0	0.72882	810
		686
		508

The generation of reflector cross-sections involves a multitude of model parameters, e.g number of reflectors to be considered, spatial extend of the geometry, degree of detail, cross-section weighting in the reflector region, calculation of reflector discontinuity factors. In order to be coherent in the comparisons in this study, the standard KMACS approach for reflectors is applied, i.e. the same axial and radial reflector 2-group data sets created with SCALE-NEWT are used in combination with all three lattice codes. Only for the calculation of the rodded radial power distributions (cf. Section III.5.), nTRACER generated reflector data is applied.

The 2D system considered for the bottom reflector consists of a full horizontal assembly model next to a homogeneous mixture of all compositions between the lowest extent of the BEAVRS core model and the bottom of the active fuel. Likewise, the top reflector model is composed of an assembly next to a homogeneous mixture of all compositions between top of active fuel and highest extent. The model of the radial reflector is depicted in Figure 3.

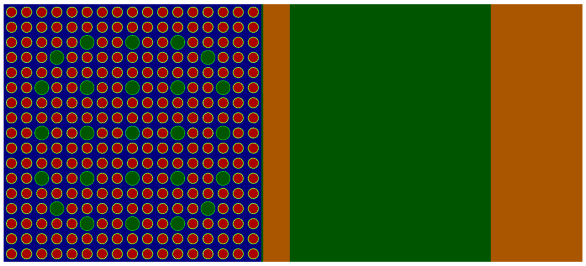

Fig. 3. Model of the radial reflector. Blue and green regions represent water with and without structure materials, orange the stainless steel structures baffle, core barrel and neutron shield.

The radial reflector model is a linear array of fuel assembly, water gap, baffle, bypass moderator and core container with reflective boundary conditions at the north, west, and south boundary as well as vacuum boundary conditions in the east. The baffle width as well as the water gap are taken directly from the benchmark description [8] (water gap: from rev. 2.0). The distance between baffle and core barrel as well as the core-barrel/neutron-shield width were chosen as the actual distance averaged over all azimuthal angles.

4. KMACS: Nodal core model

For the nodal code QUABOX/CUBBOX used within KMACS, the active core was divided axially into 34 layers and radially into nodes of ½-assembly pitch width. Thus the resulting nodes are approximately of cubic shape. The bottom-most layer has a smaller height, such that it coincides with the BA free part of the assemblies containing burnable absorbers. Figure 4 sketches the radial core layout.

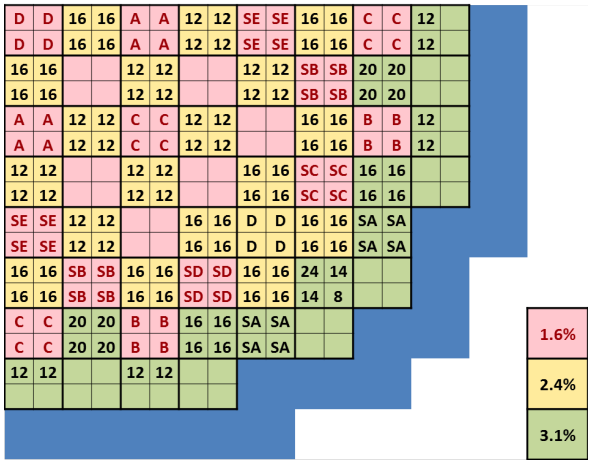

Fig. 4. Core layout within the nodal core simulator. The figure shows the south-east quadrant of the core. Colors indicate different fuel enrichments, letters the control rod banks, and numbers the number of burnable absorbers in the lattice. The blue fringe indicates the radial reflector.

The colors in the figure indicate the different enrichments of the assemblies (red: 1.6%, yellow: 2.4%, and green: 3.1% U-235). Letters indicate the control (A-D) and shutdown banks (SA-SE). Numbers indicate the number of burnable absorbers (BA) rods in the underlying lattice. Note that four boxes represent an assembly. Therefore, the assembly denoted with the numbers 24-14-14-8, effectively contains 15 burnable absorber rods which are asymmetrically arranged in the fuel assembly guide tubes. The same holds true for the assemblies denoted by 12-12-0-0, which effectively contain 6 BA rods.

The radial reflector (depicted in blue in the figure) has the same radial mesh as the fuel assemblies. The axial reflector node heights agree with the distances between active zone and highest and lowest extent, respectively.

III. RESULTS

1. Lattice multiplication factors

Table IV lists the transport multiplication factors of all lattices for each of the codes under consideration at HZP conditions and 975 ppm boron concentration.

The differences for the uncontrolled status agree with the SERPENT reference within less than 500 pcm. Differences of this order of magnitude are not unusual when comparing transport codes based on different methods and different nuclear data releases. Large deviations of more than 1000 pcm are observed for the controlled status. These require further investigation.

TABLE IV. Comparison of multiplication factors against SERPENT results for the different lattices.

Lattice	SERPENT	nTRACER	NEWT	HELIOS
1.6-0/0	0.99271	310	-16	-98
1.6-0/1	0.61825	312	931	-762
2.4-0/0	1.13502	452	-9	-171
2.4-0/1	0.74147	484	1238	-880
2.4-12/0	1.01165	364	-27	-95
2.4-16/0	0.97321	351	-16	-79
3.1-0/0	1.21710	524	-19	-253
3.1-0/1	0.82102	614	1467	-932
3.1-8/0	1.13793	488	-17	-194
3.1-12/0	1.09859	471	-14	-148
3.1-14/0	1.08146	476	3	-153
3.1-16/0	1.06115	460	0	-128
3.1-20/0	1.02552	442	4	-108
3.1-24/0	0.99131	428	17	-99

2. HZP eigenvalues

Table V lists the calculated eigenvalues for which experimental criticality $k_{\text{eff}} = 1$ was reached.

TABLE V. Deviations from criticality $\Delta\rho_i = 10^5 \times (1 - 1/k_i)$ with respect to the measurement. AVG and RMS denote the average and root-mean squared deviations.

Core status	nTRACER	NEWT	HELIOS
ARO @975 ppm	88	-329	-218
D in @902 ppm	233	-172	-83
C, D in @810 ppm	130	-249	-125
A, B, C, D in @686 ppm	-49	-396	-255
A, B, C, D, SC, SD, SE in @508ppm	-259	-522	-318
AVG	29	-333	-200
RMS	172	355	217

The SERPENT reference ARO eigenvalue is $k_{\text{eff}} = 0.99551 \pm 1$, i.e. -451 pcm off-critical. Note that this reference calculation was performed completely without control rods, whereas in KMACS the D bank was inserted 23.7cm into the core, in agreement with [8]. KMACS calculations completely without rod insertion result in a criticality increase by +4 pcm for all lattice codes.

KMACS-nTRACER slightly overestimates criticality (maximum deviation -259 pcm, average +29 pcm), whereas it is underestimated using NEWT (max. -522, avg. -333 pcm) and HELIOS data (max. -318, avg. -200 pcm).

The root-mean squared deviation from experimental criticality using KMACS is about 200-300pcm and thus, as expected, larger than for the nTRACER reference calculations

(110 pcm), listed in [9].

Thus concerning criticality, good agreement between measurement and KMACS calculations are obtained using nTRACER, while the deviations using NEWT and HELIOS are larger, but still acceptable.

3. Radial power distributions

Figure 5 shows the normalized radial power distribution obtained with SERPENT for the ARO case.

0.737	0.832	0.833	0.998	0.889	0.975	0.937	0.979
0.832	0.796	0.969	0.891	1.025	0.907	1.128	1.037
0.833	0.969	0.890	1.045	0.926	1.014	0.935	0.912
0.998	0.891	1.045	0.968	1.105	1.023	1.168	0.748
0.889	1.025	0.926	1.105	1.442	1.186	1.233	
0.975	0.907	1.014	1.023	1.186	1.224	0.899	
0.937	1.128	0.935	1.168	1.233	0.899		
0.979	1.037	0.912	0.748				

Fig. 5. SERPENT ARO radial power map.

In Figure 6, the KMACS-nTRACER, NEWT, and HELIOS assembly power results for the case completely without control rods are compared with SERPENT.

0.8%	0.5%	0.9%	0.8%	0.6%	0.0%	0.1%	-1.0%
0.5%	0.9%	0.7%	0.9%	0.5%	0.3%	-0.8%	-1.3%
0.9%	0.7%	1.0%	0.8%	0.7%	0.1%	0.1%	-0.9%
0.8%	0.9%	0.8%	1.0%	0.7%	0.7%	-0.4%	-0.9%
0.6%	0.5%	0.7%	0.7%	0.5%	1.0%	-1.0%	
0.0%	0.3%	0.1%	0.7%	1.0%	-0.1%	-2.2%	
0.1%	-0.8%	0.2%	-0.4%	-1.0%	-2.2%		
-1.0%	-1.3%	-0.9%	-0.9%				

2.8%	2.5%	2.4%	0.4%	1.2%	-0.2%	-1.2%	-0.6%
2.5%	2.6%	0.8%	1.9%	-0.4%	-0.2%	-0.8%	0.3%
2.4%	0.8%	2.2%	0.0%	0.7%	-0.5%	-1.3%	-0.6%
0.4%	1.9%	0.0%	0.7%	-0.2%	-1.0%	-1.0%	1.2%
1.2%	-0.4%	0.7%	-0.2%	-0.3%	-1.2%	-0.1%	
-0.2%	-0.2%	-0.5%	-1.0%	-1.2%	1.9%	-0.5%	
-1.2%	-0.8%	-1.3%	-1.0%	-0.1%	-0.5%		
-0.5%	0.4%	-0.5%	1.2%				

-6.3%	-6.3%	-5.3%	-4.1%	-3.3%	-2.3%	0.0%	3.1%
-6.3%	-5.7%	-4.9%	-4.1%	-2.9%	-1.7%	0.1%	3.9%
-5.3%	-4.9%	-4.2%	-3.1%	-2.1%	-1.2%	0.8%	3.7%
-4.1%	-4.1%	-3.1%	-2.0%	-0.8%	0.8%	2.6%	5.0%
-3.3%	-2.9%	-2.1%	-0.8%	2.6%	2.8%	5.7%	
-2.3%	-1.7%	-1.2%	0.8%	2.8%	4.9%	5.4%	
0.1%	0.1%	0.8%	2.6%	5.7%	5.4%		
3.1%	4.0%	3.7%	5.0%				

Fig. 6. Relative differences in assembly powers with respect to SERPENT using nTRACER (above), NEWT (middle), and HELIOS (below).

While for both nTRACER and NEWT, the assembly powers at the center of the core are higher than the reference values, for HELIOS the trend is opposite, i.e. the assembly powers at the fringe of the core are higher than the reference values. The deviations from SERPENT in assembly powers range within [-2.2%,1.0%], [-1.3%,2.8%], and [-6.3%,5.7%] for nTRACER, NEWT, and HELIOS, the RMS deviations being 0.86%, 1.11%, and 3.55%, respectively.

Whereas for nTRACER and NEWT 2-group data, good agreement between nodal and reference calculation is reached, the deviations using HELIOS 2-group data should be examined further.

4. Control rod worths

The BEAVRS benchmark lists experimentally determined control rod worths which compare criticality when subsequently inserting additional control/shutdown banks, starting from the ARO state. The same procedure was performed in KMACS simulations. Starting from the ARO state and a critical boron concentration of 975 ppm, the D, C, B, A, SE, SD, and SC banks are inserted, ending up in a configuration where only shutdown banks SA and SB are out of the core. Table VI lists the control bank worth results in comparison with the experimental data. With respect to the control bank worths, on average good agreement with the measurement is achieved for both KMACS-nTRACER and NEWT (root-mean squared deviation of the worths about 60 pcm). The corresponding value for HELIOS is larger, 95 pcm.

TABLE VI. Calculated control bank worths and reactivity differences with respect to the measurement.

CR bank	Exp.	nTRACER	NEWT	HELIOS
D	788	-1	6	2
C	1203	29	32	-36
B	1171	85	84	100
A	548	-99	-92	-171
SE	461	-86	-69	-139
SD	772	6	12	-25
SC	1099	2	-21	-56

The recent benchmark update (rev. 2.0) concerning the control rod geometry and composition is not taken into account here. It will certainly have an impact on both the control bank worths and the HZP eigenvalues of the rodded states. Yet, as many published results [9, 13] are in close range to those of KMACS, the update will assumably not effectuate qualitative changes for these integral results.

5. Radial power distributions in controlled state

On local quantities as the radial power distribution discussed in this section, the effect of a change in the control rod definition is expected to be larger. Therefore it is important to stress that for both nTRACER reference and KMACS calculation the same control rod definition of the benchmark rev. 1.1.1 is used.

As observed in Table IV, the infinite multiplication factors of the controlled lattices differ largely for the different

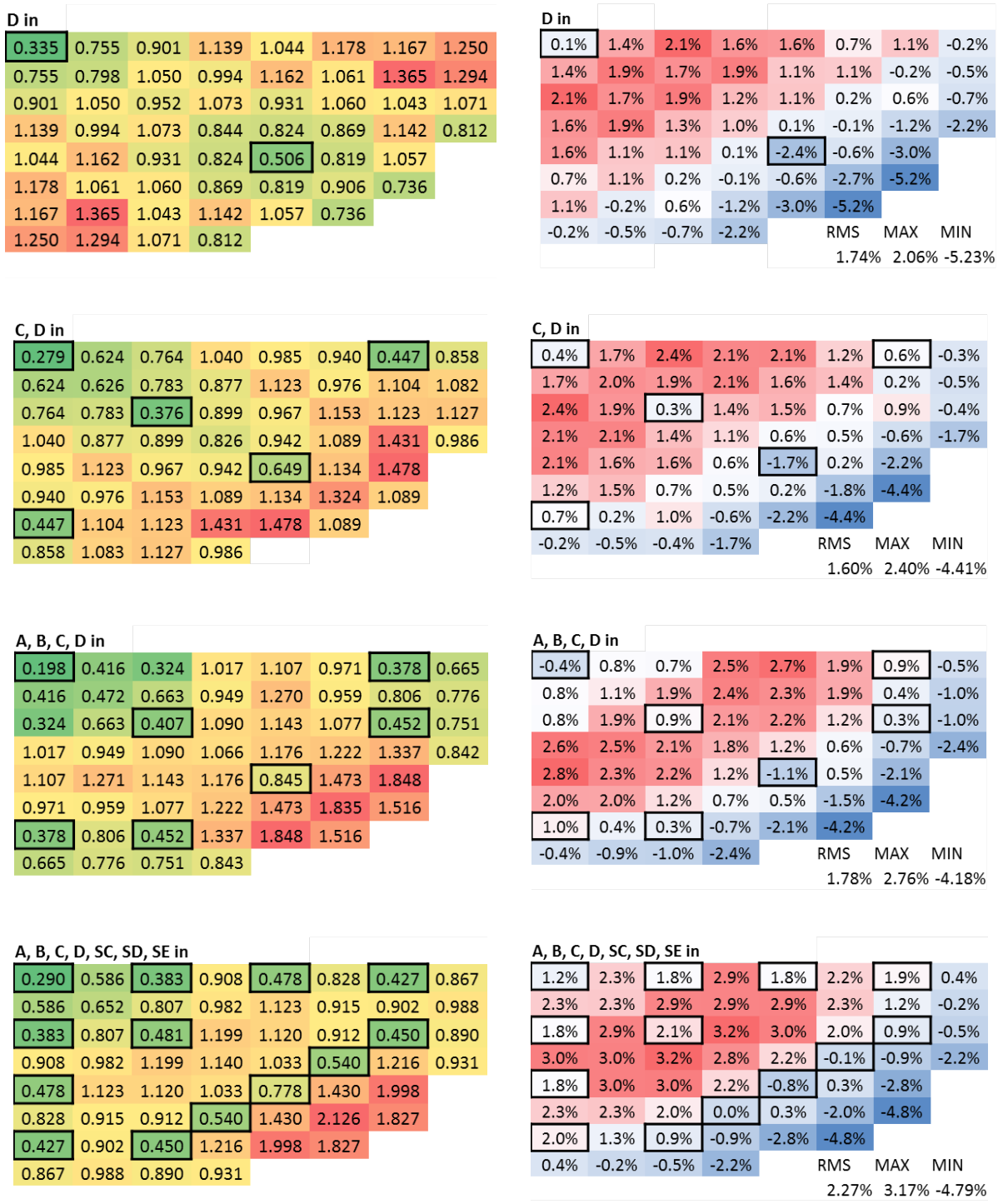

Fig. 7. Assembly power maps from rodded whole-core nTRACER calculations (left) and relative differences using KMACS-nTRACER (right). Bold boxes around the assemblies indicate rodded locations.

transport codes. Therefore, the comparison of the controlled-state power distributions is restricted to the nTRACER code, both for the reference calculation and the 2-group data generation. Within this section, also reflector data generated with nTRACER is applied. The radial reflector model is the same as depicted in Figure 3, and a single reflector data set is used at all radial reflector locations.

Figure 7 presents radial power maps from the nTRACER

reference calculation and the respective relative differences observed by KMACS-nTRACER. Considered are the four rodded critical HZP configurations of the benchmark at their respective boron concentrations, cf. Table V.

Except for the corner locations, a good quantitative agreement is observed. The RMS deviations for the four rodded configurations amount to 1.74%, 1.60%, 1.78%, and 2.27%, respectively. Specially at the control rod locations, where the power is low, the maximum and minimum deviation are only +2.1% and -2.4%. This correspond to less than 1.1% of the mean assembly power. This is a very satisfying result.

At the corners, where the largest relative differences in assembly power are observed (up to -5.2%), the core barrel comes closest to the assemblies, and the neutron shield is present, cf. Figure 1. Further investigation will show whether a more detailed radial reflector model for this location will improve the KMACS agreement with the reference solution also at these locations.

6. Isothermal temperature coefficients

For the calculation of the isothermal temperature reactivity coefficients (ITCs), all temperatures have been shifted by ±10°F = ±5.55K. Assuming constant reactor pressure, the moderator density changes accordingly, cf. Table III.

KMACS calculations have been run according to these modified core conditions, for the ARO state @975ppm boron, as well as with control bank D in @902ppm, and banks D, C in @810ppm. Table VII lists the resulting ITCs.

TABLE VII. Calculated ITCs [pcm/°F] in comparison with experimental data.

Case	Exp.	nTRACER	NEWT	HELIOS
ARO	-1.75	-2.40	-2.62	-3.82
D in	-2.75	-3.63	-5.83	-5.11
C, D in	-8.01	-8.43	-3.41	-9.87

The KMACS-nTRACER results differ by less than 1 pcm/°F from both experimental data and reference calculation. This is a satisfying result for the applied methodology. On the other hand, for KMACS-NEWT only the ARO case, and for KMACS-HELIOS none of the cases fall into this range. Here, further investigation on the temperature and density behavior of the underlying cross-sections could provide insight on the reasons of this deviations.

IV. CONCLUSIONS AND OUTLOOK

For the present paper, the HELIOS and nTRACER codes have been integrated into the modular core simulator KMACS as lattice codes for the generation of 2-group data. The new functionalities are tested and compared to the results of KMACS using SCALE-NEWT data as well as to reference calculations and measurement data. The comparison is based on the BEAVRS reactor first core.

Concerning the results of the lattice calculations, the differences in multiplication factors of uncontrolled lattices are reasonable, taking into account the different underlying nuclear data libraries. Among the considered lattice codes, nTRACER yields the closest agreement with the Monte Carlo reference for the controlled lattices.

Core calculations were performed to compare with hot zero power measurement data for the BEAVRS first core, i.e. criticality at various boron concentration and control bank insertion statuses, control bank worths and isothermal temperature coefficients. Here, good agreement between measurement and KMACS results using nTRACER and NEWT is obtained, while the HELIOS results deviate stronger.

Furthermore, the corresponding radial power distributions were compared with reference calculations. The SERPENT radial power distribution of the HZP ARO state agrees well with KMACS, both using nTRACER and NEWT, whereas larger deviations with HELIOS were observed.

The radial power distribution of the rodded HZP configurations obtained by KMACS-nTRACER were compared with reference quarter-core calculations performed with nTRACER. RMS deviations of ≤2.3% in the assembly powers were obtained and specially good agreement at the rodded assemblies. The largest deviations were found at corner assemblies close to core barrel and neutron shield where the KMACS reflector model is a coarse approximation.

In all, whereas this first application of HELIOS-produced 2-group data in KMACS has not been satisfactory, nTRACER as lattice code within KMACS has proven to produce good results for all simulations performed within the scope of this paper.

For cycle depletion calculations, KMACS requires 2-group data functionalized according to burnup. For the validation of this feature in KMACS-nTRACER, the BEAVRS cycle 1 depletion calculation is planned.

V. ACKNOWLEDGMENTS

We acknowledge Min Ryu for providing us with nTRACER whole core BEAVRS results.

This work was supported by the German Federal Ministry for the Environment, Nature Conservation, Building and Nuclear Safety.

REFERENCES

1. M. ZILLY, A. AURES, M. KÜNTZEL, I. PASICHNYK, Y. PÉRIN, A. SEUBERT, K. VELKOV, and W. ZWERMANN, "Erstellung und Qualifizierung eines nuklearen Kernsimulators für die Sicherheitsbewertung aktueller Reaktorkernbeladungen," Tech. rep., GRS (2015).
2. M. ZILLY, M. KÜNTZEL, A. AURES, V. HANNSTEIN, K. VELKOV, and A. PAUTZ, "KMacs, a modular adaptable core simulator," *Proc. PHYSOR 2016*, Sun Valley, ID, USA, May 1–5, 2016.
3. J. BOUSQUET, M. ZILLY, and J. TAFOREAU, "Analysis of the Hot Zero Power of the BEAVRS benchmark using the DRAGON/PARCS and the SCALE6.2/QUABOX-CUBBOX codes sequences," *EUROSAFE ETSON AWARD Paper* (2016).
4. Oak Ridge National Laboratory, *SCALE: A Comprehensive Modeling and Simulation Suite for Nuclear Safety*

Analysis and Design (Version 6.2.1, 2017), ORNL/TM-2005/39.

5. Y. S. JUNG, C. B. SHIM, C. H. LIM, and H. G. JOO, "Practical numerical reactor employing direct whole core neutron transport and subchannel thermal/hydraulic solvers," *Ann. Nucl. Energy*, **62**, 357 (2013).
6. Y. S. BAN and H. G. JOO, "Leakage correction of homogenized few-GCs through functionalization on leakage fraction," *Proc. PHYSOR 2016*, Sun Valley, ID, USA, May 1–5, 2016.
7. Studsvik Scandpower, *HELIOS Methods* (Version 1.12, 2012).
8. N. HORELIK, B. HERMAN, B. FORGET, and K. SMITH, "Benchmark for Evaluation and Validation of Reactor Simulations (BEAVRS)," *Proc. M&C 2013*, Sun Valley, ID, USA, May 5–9, 2013, rev. 1.1.1.
9. M. RYU, Y. S. JUNG, H. H. CHO, and H. G. JOO, "Solution of the BEAVRS benchmark using the nTRACER direct whole core calculation code," *J. Nucl. Sci. Technol.*, **52**, 961 (2015).
10. S. LANGENBUCH and K. VELKOV, "Overview on the Development and Application of the Coupled Code System ATHLET-QUABOX/CUBBOX," *Proc. M&C 2005*, Avignon, France, September 12–15, 2005.
11. Y. TAHARA, T. KANAGAWA, and H. SEKIMOTO, "Two-Dimensional Baffle/Reflector Constants for Nodal Code in PWR Core Design," *J. Nucl. Sci. Technol.*, **37**, 986 (2000).
12. National Institute of Standards and Technology, *Thermophysical Properties of Fluid Systems*, http://webbook.nist.gov/chemistry/fluid/, retrieved February, 2017.
13. D. J. KELLY, III, B. N. AVILES, and B. R. HERMAN, "MC21 Analysis of the MIT PWR Benchmark: Hot Zero Power results," *Proc. M&C 2013*, Sun Valley, ID, USA, May 5–9, 2013.